

Experimental analysis of the Strato-rotational Instability in a cylindrical Couette flow

M. Le Bars and P. Le Gal

*Institut de Recherche sur les Phénomènes Hors Equilibre,**UMR 6594, CNRS & Aix-Marseille Université, 49 rue F. Joliot-Curie, BP146, 13384 Marseille Cédex 13*

(Dated: October 30, 2018)

This study is devoted to the experimental analysis of the Strato-rotational Instability (SRI). This instability affects the classical cylindrical Couette flow when the fluid is stably stratified in the axial direction. In agreement with recent theoretical and numerical analyses, we describe for the first time in detail the destabilization of the stratified flow below the Rayleigh line (i.e. the stability threshold without stratification). We confirm that the unstable modes of the SRI are non axisymmetric, oscillatory, and take place as soon as the azimuthal linear velocity decreases along the radial direction. This new instability is relevant for accretion disks.

PACS numbers: 47.20.Ft; 47.20.Qr; 97.10.Gz

Taylor-Couette flow (or cylindrical Couette flow) is certainly one of the most popular laboratory flows and its study has already led to an abundant scientific literature. Several articles review the theoretical and experimental features of this flow that consists of a simple shear between two co-axial rotating cylinders [1]. Its linear stability is given by the Rayleigh criterion which states that rotating shear flows are stable when their angular momentum increases radially. The richness of the transition diagram that reports the different flow patterns and their subsequent transitions to chaos and turbulence has been extensively explored by Andereck et al. [2]. Amazingly, the literature about Taylor-Couette flows in the presence of an axial stable stratification is much more limited even though it finds direct applications in geophysics (atmospheric or oceanic flows) or astrophysics (accretion disks for instance). The first experiment on stratified Taylor-Couette flow was performed by Thorpe [3] in 1966. His results were further extended by the experiments of Withjack and Chen [4], Boubnov et al. [5], Caton et al. [6] and by the numerical simulations of Hua et al. [7]. Most of these studies were performed with a stationary outer cylinder and all concluded that stable vertical stratification stabilizes the flow and reduces the axial wavelength of the unstable modes which bifurcate through Hopf bifurcations.

In astrophysics, Keplerian flows whose angular velocity is $\Omega(r) \sim r^{-3/2}$, are always stable to infinitely small perturbations in respect to the Rayleigh criterion [8]. As a consequence of this stability, several scenarios have been recently proposed to justify the existence of turbulence in accretion disk flows. Ingredients other than pure shear then need to be taken into account in order to trigger instabilities and transition to turbulence in these flows. One of the most popular scenarios relies on the Magneto-Rotational Instability [9] but other instabilities such as the elliptical instability [10] or non linear shear instabilities [8] have also been suggested.

In 2001, Molemaker et al. [11] and Yavneh et al. [12]

predicted that cylindrical Couette flows in a stratified fluid may become unstable even if the Rayleigh criterion for stability was verified, i.e. in the corresponding stable regime of pure fluid flow. Moreover, and contrary to the classical Taylor vortices of the centrifugal instability, the most unstable modes should be non-axisymmetric. This theoretical analysis has then been continued in an astrophysical context by Shalybkov and Rüdiger [13] and extended to the stability of accretion disk Keplerian flows by Dubrulle et al. [14] who gave to this new instability its now accepted appellation Strato-Rotational Instability (SRI). To the best of our knowledge, and despite explicit calls recently published [11, 13], no experimental validation of these theoretical predictions has yet been provided, apart from a short comment made by Withjack and Chen [4] in 1974 and a stability curve that was determined by Boubnov and Hopfinger in 1997 [15]. We present here the first quantitative experimental evidences of the Strato-rotational Instability and its expected helicoidal modes.

Our study is based on Kalliroscope visualizations performed in a classical Couette device with a ratio of inner to outer cylinder diameters equal to $\eta = 0.80$. The shear created by the differential rotation of these cylinders is measured by the ratio μ of the outer cylinder rotation speed to the inner cylinder rotation speed: $\mu = \frac{\Omega_o}{\Omega_i}$. Using μ and η , the two traditional control parameters for the cylindrical Couette flow, the Rayleigh criterion reads $\mu = \eta^2$ which is represented by the Rayleigh line in the (Ω_o, Ω_i) plane. A salt stratification is realized along the axis of rotation of the Couette apparatus using the classical "double-bucket" filling method [16]. The corresponding Froude number of the fluid is chosen equal to 0.5 which is the estimated value for accretion disks [14]. Contrary to the extensive study of Caton et al. [6] where the outer cylinder is at rest, the particularity of our study comes from the possibility to rotate separately both cylinders and therefore to study the development of non axisymmetric helicoidal modes in usually stable

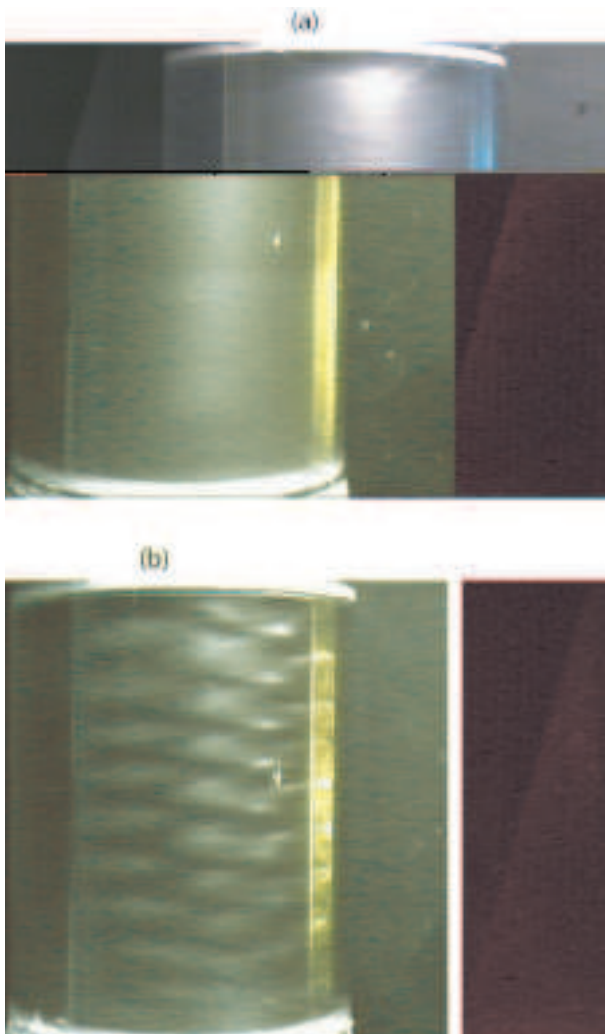


FIG. 1: Kalliroscope visualization of the stable Couette flow in pure water (a) and of the SRI in the vertically stratified salt water with $Fr = 0.5$ (b) at the same Reynolds number $Re = 1155$ ($\Omega_o = 1.07 rad/s$, $\Omega_i = 1.5 rad/s$). The braid pattern of the SRI is formed by the superimposition of two identical helicoidal waves (azimuthal wavenumber $m = 4$) propagating in opposite vertical directions. The laser sheet shows the meridional section of the travelling pattern (on the right part of the device).

regions (see fig. 1). As we will see, our experimental determination of the Strato-rotational Instability threshold is in excellent agreement with the value $\mu = \eta$ proposed in [13] and corresponding to a constant azimuthal linear velocity along the radial direction.

Our Couette device consists of two co-axial cylinders whose length is $168mm$. The inner radius of the outer cylinder is $R_o = 69mm$ and the radius of the inner cylinder is $R_i = 55mm$, conferring a $14mm$ gap between the two concentric cylinders. The ratio of the inner to outer radius of the fluid cavity is equal to $\eta = 0.8$ explicitly chosen to allow some comparisons with the results

of Shalybkov and Rüdiger [13]. The cylinders are positioned vertically. The inner cylinder is made of black polished acetal plastic and the outer one is of transparent glass so visualizations can be performed with the help of Kalliroscope flakes. To complement these bulk visualizations that use a classical light bulb for illumination, a laser sheet can also be installed to get a description of the hydrodynamical structure in a vertical meridional plane (see figure 1). The cylinders are driven by a d.c. servo-motor. Rotational speeds are measured by an optical encoder with an accuracy better than 1%. The top and bottom lids of the device are fixed to the external cylinder and rotate with it. The experimental protocol is the following. The classical double-bucket technique [16] is used to obtain a vertical stratification of salt water. The vertical density gradient is measured before each run with the help of a density meter or a conductivity meter using a calibrated plunging probe. A linear gradient is quite easily achieved and its value leads to the determination of the Brunt-Väisälä pulsation: $N = (-\frac{g}{\rho} \frac{\partial \rho}{\partial z})^{1/2}$ with an accuracy better than 5 %. When changing the salt concentration in one of the filling bucket, N can be chosen between 0 and $3.1 rad/s$. The Froude number Fr is then calculated by the ratio of the inner cylinder rotation speed Ω_i to N . We have fixed a priori its value to $Fr = 0.5$ in order to compare our experimental results with the numerical predictions of [13]. Once the density gradient is established, the inner cylinder rotation speed Ω_i is thus fixed for each run, which also fixes the value of the Reynolds number: $Re = \frac{\Omega_i R_i (R_o - R_i)}{\nu}$, where ν is the viscosity of water. For each run, the initial condition is solid body rotation obtained when both cylinders rotate at the same speed, then we systematically change the angular velocity ratio $\mu = \frac{\Omega_o}{\Omega_i}$ by slowly decreasing Ω_o . When the threshold for the SRI is reached a single travelling helicoidal wave appears in the flow. After some minutes, a vertical counter propagative wave, having identical azimuthal, temporal and vertical (in absolute value) frequencies is superimposed on the first one, and creates a braid pattern as illustrated in figure 1-b). We believe that the initial dissymmetry between both waves comes from initial conditions and that the reflection on the lids of the first wave restore the symmetry between $+k$ and $-k$ waves expected from the theory. Figure 1-a) shows the pure water cylindrical Couette flow in the exact same conditions and demonstrates the stability of the flow in the absence of stratification. Let us note that whereas it is known that stratification damps vertical motions and instabilities in some cases [3, 6, 7, 15], it is quite clear here that it can also destabilize shear flows.

Ten series of experiments corresponding to ten different Reynolds numbers ranging from 339 to 1210 have been performed. Figure 2 summarizes the experimental stability diagram of the flow in the parameter plane (μ, Re) . It shows our experimental data points (\times for instability, \circ for stable flow) superimposed on the stability diagram calculated in [13]. As can be observed an excellent agreement is obtained. In particular, we confirm that the

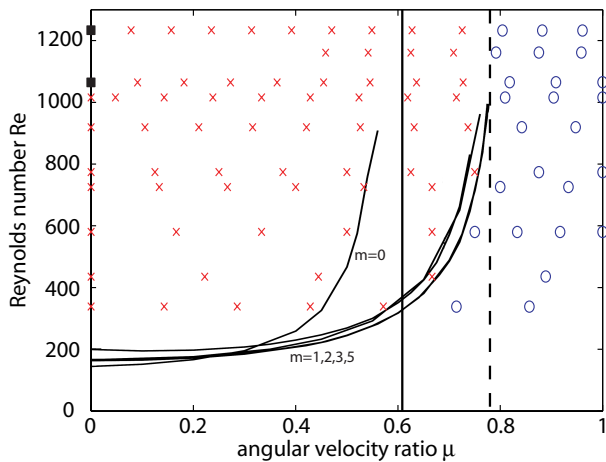


FIG. 2: Stability diagram of the Strato-Rotational Instability in the (Re, μ) parameter plane for a Froude number of 0.5 obtained for N ranging from 0.85 rad/s to 3.1 rad/s . \circ and \times stand respectively for experimental observations of stable and unstable flows. Squares stand for stationary axisymmetric Taylor vortices. These experimental data points are superimposed on the solid lines of the theoretical stability diagram of Shalybkov and Rüdiger [13] for azimuthal wavenumbers $m = 0$ (e.g. the classical Taylor vortices) and $m = 1, 2, 3, 5$ for $\eta = 0.78$ (some helicoidal modes of the SRI). Vertical lines correspond to the theoretical inviscid limits with respectively the Rayleigh line $\mu = \eta^2$ relevant for the unstratified case (solid line) and the threshold for the stratified case $\mu = \eta$ as suggested in [13] (dotted line).

inviscid threshold, proposed by Shalybkov and Rüdiger [13], is given by $\mu = \eta$. Further decreasing μ , patterns become increasingly complex as additional helicoidal modes ($m \neq 0$) are progressively added. We suggest that the helicoidal modes calculated by Molemaker et al. [11] and Shalybkov and Rüdiger [13] and observed in our experiments should be by continuity the "vortex modes" described by Caton et al. [6] when the outer cylinder does not rotate. We never found the "standing wave" regime of Caton et al. [6] (i.e. their pulsating axisymmetric modes) within the explored range, presumably because its unstable region is too narrow and our experimental device is not precise enough to excite this very marginal state (see the comparison between the results of [5] and [6]). Nevertheless, in experiments at $\mu = 0$ and large Reynolds number, we observed the reappearance of stationary axisymmetric Taylor vortices in agreement with the regime diagram of Boubnov et al. [5]. This stationary axisymmetric mode was never excited when decreasing μ for $\mu > 0$, but once excited at $\mu = 0$, they could then be maintained up to $\mu = 0.2$. These interesting non-linear effects are beyond the scope of the present paper devoted to the SRI and will be further studied. Figure 3-a) shows the space-time diagram of the braid pattern observed at SRI threshold and shown in figure 1-b). These diagrams are built by assembling vertical lines from successive video images, and allow to extract in a systematic

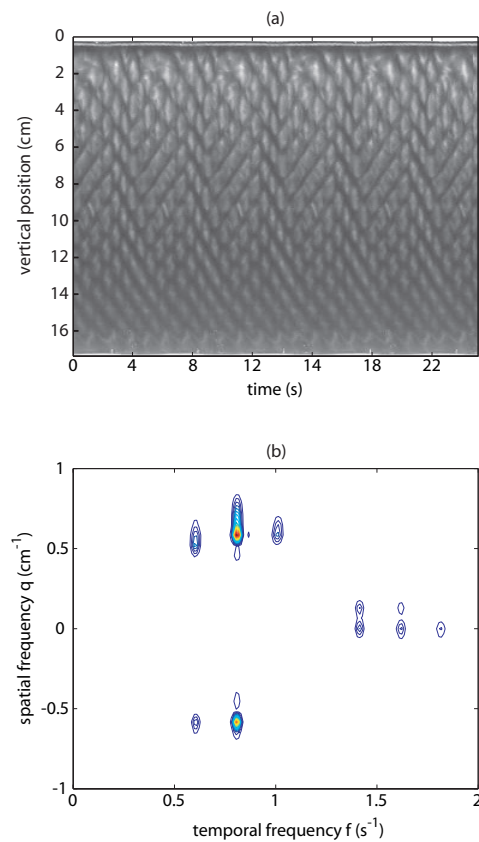


FIG. 3: (a) Space-time diagram at threshold of the growing helicoidal mode presented in figure 1-b), with $Fr = 0.5$ and $Re = 1155$. (b) 2D-Fourier Power spectra of the space-time diagram: contours are equally spaced from 0 to the maximum energy E^{max} with a spacing of $E^{max}/20$. Non linear interaction between both helicoidal waves is visible as peaks around $q \simeq 0$ and $f \simeq 1.6 \text{ s}^{-1}$.

way the temporal frequency f and the axial frequency q of the hydrodynamic structures using a 2D-Fourier transform, as shown in figure 3-b). At instability threshold, we systematically recover two symmetrical points (f, q) and $(f, -q)$ corresponding to the two helicoidal modes forming the braid pattern. Further away from the threshold, the 2D-Fourier transforms are more complex and indicate other peaks, but in the following we only focus on the most energetic of them. As suggested by the analytical study of Shalybkov and Rüdiger [13], we did not observe any systematic variation of the wavenumber $k = 2\pi q (R_i(R_o - R_i))^{1/2}$: over all our experiments, we measure a mean value of 10.6 with a standard variation of 1.5 in close agreement with analytical and numerical results [12, 13]. This value corresponds to a wavelength equal to 1.17 time the gap, smaller than the standard value in the absence of stratification (i.e. twice the gap) and confirms the reduction of the vertical extension of the structures because of stratification. Figure 4-a) presents the evolution of the experimentally determined pulsation $\omega = 2\pi f/\Omega_i$ divided by the mean normalized angular velocity, as a function of μ . As can be observed, the data points are clustered along horizontal lines corresponding

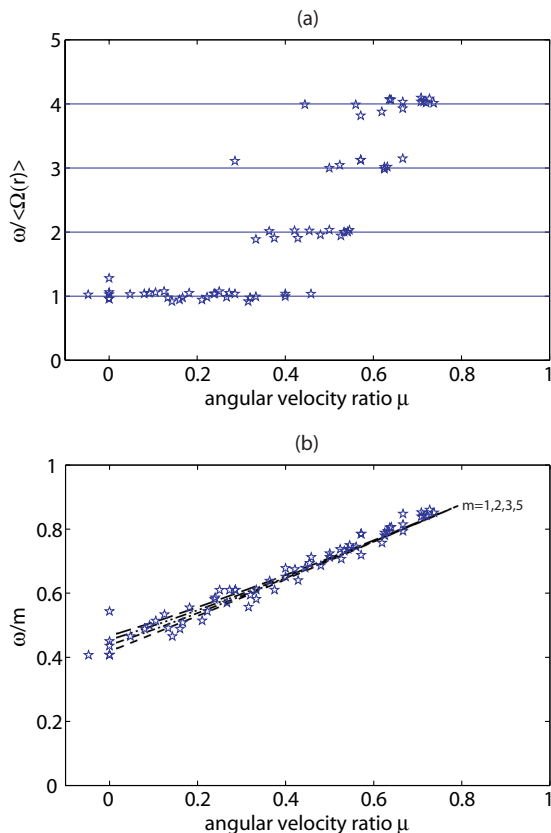


FIG. 4: (a) Evolution of the pulsation ω of the prevalent helicoidal mode divided by the mean angular pulsation $\langle \Omega(r) \rangle$ for $Fr = 0.5$ obtained for N ranging from 0.85 rad/s to 3.1 rad/s : all ratios align with integer values as expected from the azimuthal periodicity in the cylindrical geometry. These are highlighted by horizontal lines and correspond to the azimuthal wavenumber m (from 1 to 4) of the selected mode. These values are used in (b) to rescale ω . All experimental data points correctly aligns with the analytical predictions (dotted lines) of the SRI [13].

to integer values. Indeed, extending the simple advection argument given by Caton et al. [6] to $\mu > 0$, one can estimate that the helicoidal patterns are simply advected at the mean angular velocity $\langle \Omega(r) \rangle$ of the fluid between the cylinders. Hence the ratio $\omega / \langle \Omega(r) \rangle$ actually indicates the azimuthal wavenumber m of the selected mode, ranging from $m = 1$ to $m = 4$. We confirm these conclusions by directly measuring the azimuthal wavenumber at threshold when there is a single helix in the flow. In figure 4-b), we then compare our experimental results using the previously determined m with the numerical results of [13]. Again, perfect agreement is found.

In conclusion, we have extended previous experimental studies of stratified Taylor-Couette flow by a systematic exploration of the stable range according to the Rayleigh criterion. We have observed the new Strato-rotational Instability in the form of non-axisymmetric oscillating modes. Our results validate the theoretical results of Molemaker et al. [11], Yavneh et al. [12], Shalybkov and Rüdiger [13] and Dubrulle et al. [14]. In particular, instability thresholds, axial and azimuthal wavenumbers and temporal frequencies of the helicoidal travelling modes ($m \neq 0$) have been measured for a fixed Froude number $Fr = 0.5$, an aspect ratio $\eta = 0.80$ and for different Reynolds numbers. Comparisons with theoretical predictions [13] are excellent. Moreover, let us emphasize that in the inviscid limit, the SRI threshold tends to the value $\mu = \eta$, contrary to $\mu = \eta^2$ given by the Rayleigh criterion valid in the unstratified case. As already remarked by Shalybkov and Rüdiger [13], this implies that stratified Keplerian flows such as those found in accretion disks and characterized by $\Omega(r) \sim r^{-3/2}$ (i.e. $\mu_{Kepler} = \eta^{3/2}$) are stable following the Rayleigh criterion (i.e. $\mu_{Kepler} > \eta^2$), but can be destabilized by the SRI as $\mu_{Kepler} < \eta$.

Acknowledgements:

The authors are grateful to J. Caillet, M. Borel and M. Vial-Sablier for their help during the experiments.

-
- [1] R.C. Di Prima and H.L. Swinney, in Topics in Applied Physics **45**, Edts. H.L. Swinney and J.P. Gollub, Springer-Verlag, Berlin, 139 (1981). R. Tagg, Nonlin. Sci. Today **4**, 1 (1994).
 - [2] C.D. Andereck, S.S. Liu and H.L. Swinney, J. Fluid Mech. **164**, 155 (1986).
 - [3] S. A. Thorpe, Notes on 1966 Summer Geophysical Fluid Dynamics (Woods Hole Oceanographic Institute, Woods Hole, MA, 1966), p. 80.
 - [4] E.M. Withjack and C.F. Chen, J. Fluid Mech. **66**, 725 (1974).
 - [5] B.M. Boubnov, E.B. Gledzer, and E.J. Hopfinger, J. Fluid Mech. **292**, 333 (1995).
 - [6] F. Caton, B. Janiaud and E. J. Hopfinger, J. Fluid Mech. **419**, 93 (2000).
 - [7] B. L. Hua, S. Le Gentil and P. Orlandi, Phys. Fluids **9**, 365 (1997).
 - [8] B. Dubrulle, O. Dauchot, F. Daviaud, P.Y. Longaretti, D. Richard and J.P. Zahn, Physics of Fluids **17**, 095103 (2005).
 - [9] S.A. Balbus and J.F. Hawley, Rev. Mod. Phys. **70**, 1 (1998).
 - [10] N.R. Lebovitz and E. Zweibel, The Astrophys. J. **609**, part 1, 301 (2004).
 - [11] M.J. Molemaker, J.C. McWilliams and I. Yavneh, Phys. Rev. Lett. **86**, 5270 (2001).
 - [12] I. Yavneh, J.C. McWilliams and M.J. Molemaker, J. Fluid Mech. **448**, 1 (2001).
 - [13] D. Shalybkov and G. Rüdiger, J. Phys. **14**, 128 (2005); Astron. Astrophys. **438**, 411-417 (2005).
 - [14] B. Dubrulle, L. Marié, Ch. Normand, D. Richard, F. Hersant and J.-P. Zahn, Astron. Astrophys. **429**, 1 (2005).
 - [15] B.M. Boubnov and E.J. Hopfinger, Physics-Dokady **42** (6), 312 (1997).
 - [16] G. Oster, Sci. Am. **213**,70 (1965).